Noise and Vibration: *Emerging Methods*
NOVEM 2012
1-4 April 2012 Sorrento

MODELING VIBRATION TRANSMISSION IN GEARBOX/SHAFTING SYSTEMS USING AN AUGMENTED COMPONENT MODE SYNTHESIS APPROACH

Stephen A. Hambric[1], Micah R. Shepherd[1] and Robert L. Campbell[1]

[1]Applied Research Lab, Penn State University
PO Box 30, State College, Pennsylvania, USA
Email: sah19@arl.psu.edu

ABSTRACT

Transmission gearboxes are comprised of rotating shafts and gears and stationary housings. The vibrations in the rotating parts induce vibration in the housing by transmitting forces and moments through the bearings. The bearing impedances, and therefore the force transmission, depend strongly on the operating conditions of the gearbox (torque and speed). To efficiently model the force transmission for multiple operating conditions and design configurations, a component mode synthesis (CMS) approach is demonstrated for a simple test gearbox. Shaft and housing normal modes are coupled at the bearing locations using computed bearing impedance matrices. Since using conventional CMS leads to poor convergence, two augmentations to the methodology are applied: (1) use of mean bearing impedances at each connection when computing the normal modes, and (2) inclusion of static residual vectors in the modal summation. Corrections to the mean impedances are applied in the CMS to model the actual non-symmetric bearing impedances in the final solution. A simple example demonstrates the significantly improved convergence characteristics of the augmented CMS method.

1 INTRODUCTION

Vehicles and rotorcraft are powered by drive systems comprised of complex transmissions, which contain sets of gears and shafts supported by bearings. As the gears rotate at high rates of speed under high torques, they generate vibrations at multiples of Gear Meshing Frequency (GMF). The vibrations pass through the gear shafts, through the bearings, and into the transmission housing, which in turn radiates sound at the GMF frequencies.

Transmissions typically contain either rolling element bearings (ball or roller), or journal bearings. Journal bearings (JBs) support loads through extremely thin fluid films between the rotating shaft and stationary bearing. Rolling element bearings (REBs) support loads mechanically, through balls or rollers mounted between inner and outer rings. While REBs are generally more stable (JBs can experience instabilities at specific loading and rotational conditions), they are also thought to be more efficient transmitters of vibration energy, as their mechanical impedances are nearly purely spring-like. JBs, however, provide both stiffness and damping due to viscous behaviour in the fluid films. In some cases, the

fluid film damping may help dissipate some of the vibrational energy passing through the bearing.

Numerical models of transmissions [1-7] may be used to assess the potential benefits of replacing REBs with JBs. Finite Element (FE) models of shafts and housings may be coupled via the mechanical impedances of the bearings that connect them. Dynamic loads, which model the gear tooth transmission errors, placed at the locations of meshing gear teeth may be used to drive the assembled model, and vibrations on the housing may be monitored. The sound radiated by the transmission housings can be modeled using Boundary Element (BE) techniques, where a BE mesh surrounds the FE model of the gearbox housing [8].

While the common approach to assessing different bearing designs is to analyze separate FE models of gearboxes, each with different bearing impedances, this approach is computationally inefficient, and does not allow rapid assessment of the effects of changing bearings. Also, since the impedances of all bearings vary with load condition (torque), and the impedances of journal bearings also vary with rotational speed and lubricant temperature, a prohibitive number of FE models and analyses would be required to generate accurate gearbox noise spectra. Clearly, a more computationally efficient modeling approach is required.

Component mode synthesis (CMS) [9-11] allows a simple, efficient means of coupling the shafts and housing via their component modes. In CMS, the amplitudes of the component modes required to satisfy continuity of displacements at the connections between the shafts and housing are solved for. Typically, component modes with free boundary conditions are used in CMS, although modes with other boundary conditions may also be applied. However, the CMS approach can have difficulty converging to accurate solutions due to modal truncation errors when an insufficient number of modes is used in the analysis [12]. For many problems the number of modes required to obtain accurate solutions can be prohibitive.

Fortunately, a simple approach which uses residual vectors to approximate the static effects of high frequency modes on the CMS solution is available in the NASTRAN commercial finite element software [13]. The residual vectors are computed by applying static loads at all interface locations, and at all points where forces will be applied. The resulting displacement fields are modified by subtracting the contributions from the modes which are included in the CMS solution, leaving behind the static terms from all high-frequency modes which are excluded. These residual vector ‘modes’ are then added to the group of actual modes, and included in the CMS analysis, dramatically improving solution convergence and accuracy.

While the CMS approach is well established, further improvement in convergence is possible by using component modes which have more representative boundary conditions. The bearing impedances over a range of operating conditions may be examined, and a mean set of impedances applied between the shafting and bearings. The mean impedances lead to component mode shapes which are much closer to those of the actual modes. The differences between the actual and mean impedances are then applied during the CMS. This approach allows for rapid analyses over a range of bearing types, loading conditions, and rotational speeds, as the impedance deltas are easily applied.

In this paper, we demonstrate the augmented CMS procedure on a simplified version of a United States National Aeronautic and Space Administration (NASA) gearbox.

2 NASA GRC GEARBOX

A schematic of a single-reduction gearbox from NASA Glenn Research Center (NASA GRC) with key dimensions is shown in Figure 1 and described further in Table 1. Two identical spur gears are mounted to the shafts (see Figure 2), which are supported at both ends by bearings within the housing. In its default condition, ball bearings (SKF Explorer 6205)

support the shafts at their loaded ends, and roller bearings (FAG N205E) are used at the free ends. Journal bearings replaced the ball bearings for tests conducted in 2008 and 2009. The input and output shafts are connected to larger external shafts via flexible couplings. The gearbox is a simple rectangular steel box, with a flat plate bolted to its top on a stiff mounting flange. An O-ring is sandwiched between the top plate and flange within a groove machined into the top plate. The top mounting flange and all of the walls are 0.25" thick. More details on the test rig may be found in [14].

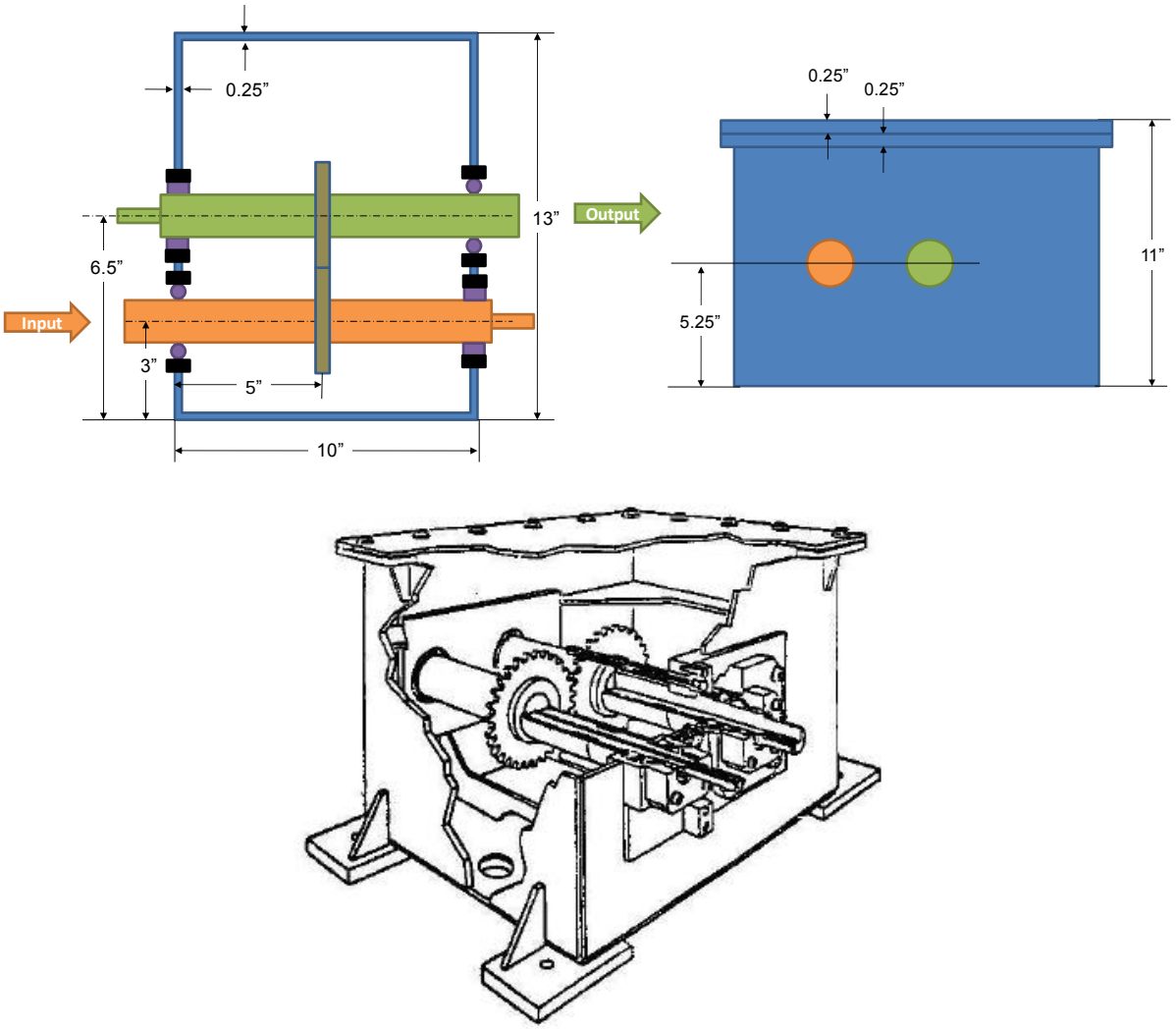

Figure 1: Schematic of NASA GRC test gearbox. Left - top view with lid cut away; Right - side view.

Height (in)	11
Width (in)	10
Length (in)	13
Wall thickness (in)	0.25
Lid thickness (in)	0.25
Material	Steel
Mean Shaft Diameter (in)	1.19

Table 1: NASA GRC test gearbox dimensions and materials.

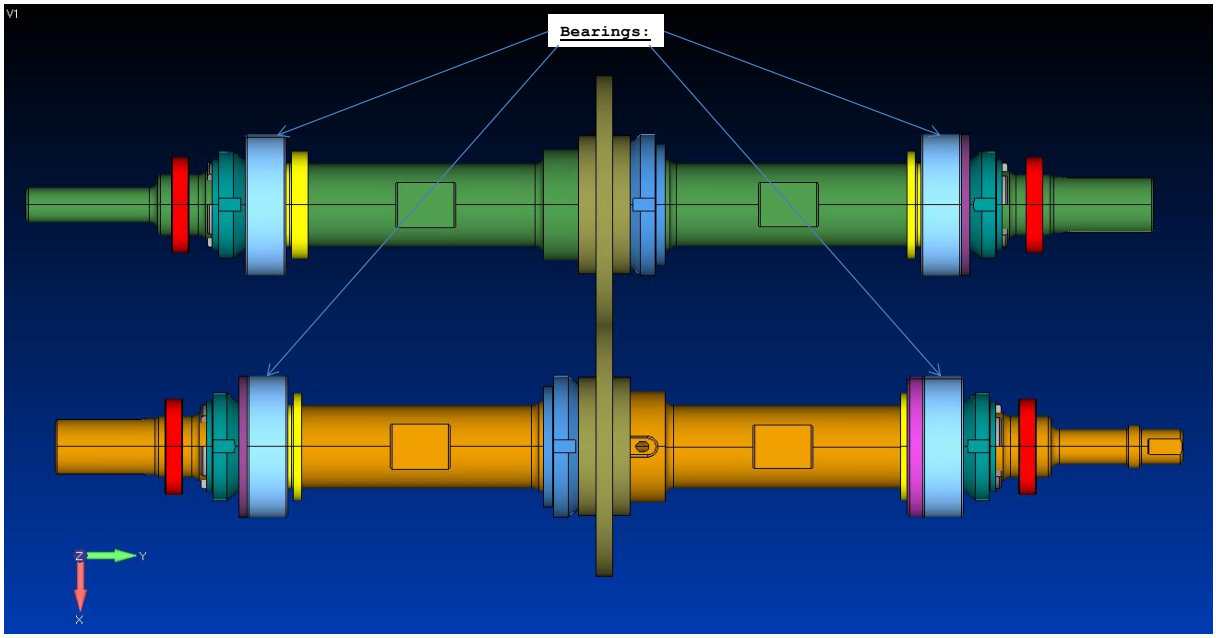

Figure 2: Shafting with rolling element bearings.

3 BEARING IMPEDANCES

Rolling element bearings or JBs couple the shafts and housings via transverse and rotational stiffness and damping coefficients. Figure 3 shows a ball bearing schematic, along with its force-displacement relationships. Transverse and rotational (moment) stiffnesses exist for all except the shaft-rotation degree of freedom. The cross terms are important, and cannot be ignored.

As a rolling element, like a ball or roller, is loaded, a portion of its surface undergoes Hertzian deformation. As the load increases, more of the surface area deforms. Since the balls and rollers are not flat, the amount of surface under deformation does not increase linearly with loading. Also, as loading increases more balls and rollers are deformed, further complicating the relationships between load and deformation (and therefore stiffness). The Lim/Singh/Liew [15, 16] approach to simulating contact deformation was implemented and used to compute the REB stiffnesses, including moment stiffnesses and cross-terms.

$$\begin{Bmatrix} F_x \\ F_y \\ F_z \\ M_x \\ M_y \\ M_z \end{Bmatrix} = \begin{bmatrix} k_{xx} & k_{yx} & k_{zx} & k_{\theta_x x} & k_{\theta_y x} & 0 \\ k_{xy} & k_{yy} & k_{zy} & k_{\theta_x y} & k_{\theta_y y} & 0 \\ k_{xz} & k_{yz} & k_{zz} & k_{\theta_x z} & k_{\theta_y z} & 0 \\ k_{x\theta_x} & k_{y\theta_x} & k_{z\theta_x} & k_{\theta_x\theta_x} & k_{\theta_y\theta_x} & 0 \\ k_{x\theta_y} & k_{y\theta_x} & k_{z\theta_x} & k_{\theta_x\theta_y} & k_{\theta_y\theta_y} & 0 \\ 0 & 0 & 0 & 0 & 0 & 0 \end{bmatrix} \cdot \begin{Bmatrix} \delta_x \\ \delta_y \\ \delta_z \\ \beta_x \\ \beta_y \\ \beta_z \end{Bmatrix}$$

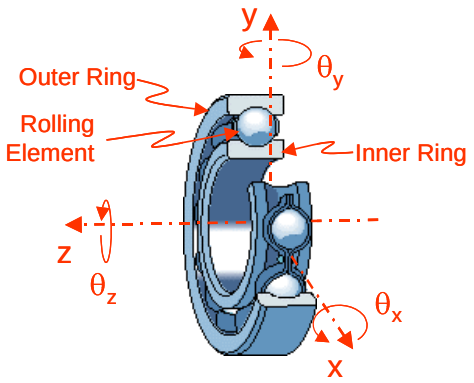

Figure 3: Ball bearing schematic and force-displacement relationships.

Journal bearings (see schematic in Figure 4) support loads through a fluid film between the shaft and bearing surfaces. As the shaft rotates, a shear layer is formed in the fluid film which supports the load. An extension to the method described by Campbell [17]

was used for the journal bearings calculations. In Campbell's approach, the pressure field in the fluid film between the shaft and bearing surface is computed by solving the Reynolds equation using finite difference methods. The external load that can be supported by the bearing is calculated by integrating the pressure over the film surface. The dynamic stiffness and damping coefficients are then related to the reaction forces by a Taylor series expansion. The circumferentially varying stiffness and damping can then be integrated to compute the overall impedances in the vertical and horizontal directions.

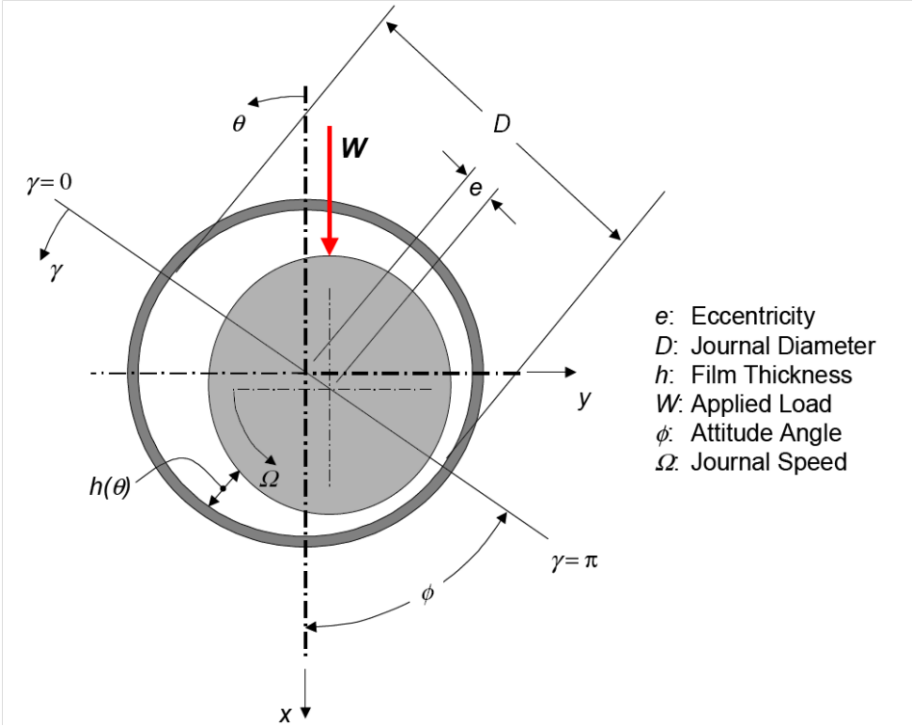

Figure 4: Journal bearing schematic and variables (film gap size is greatly exaggerated).

Moment stiffnesses and damping of the journal bearings were computed using a numerical perturbation technique. The bearing forces and moments were computed for a prescribed journal location and then the journal location was perturbed in both translational and rotational directions and the forces and moments recomputed. The secant method is then used to estimate the slope of the load-deflection curve (i.e., the stiffness). The moment damping terms cannot be so easily computed, however, and were estimated based on the ratios of the translational damping and stiffness terms. The stiffness and damping are integrated around the bearing circumference to compute total vertical and horizontal impedances for both direct and cross terms. Bearing impedances were computed for a torque of 700 in-lb and the properties shown in Table 2 (see [14] for all of the matrix terms).

Fluid viscosity	μ = 0.0294 Pa s
Fluid density	ρ = 980 kg/m^3
Journal diameter	D = 0.03195 m
Radial clearance	C = 15 µm
Bearing length	L = 0.019882 m

Table 2: Journal bearing parameters.

Figures 5 and 6 compare the total radial stiffness and moment stiffness (magnitude of the *x* and *y* components) for journal bearings as a function of rotational speed for a torque of 700 in-lb. Also shown on the plots are the radial and rotational stiffnesses for the ball and roller bearings on the input side of the gearbox. In the translational direction, the roller bearings are stiffer than the journal (and ball) bearings. Finally, the journal bearing radial stiffness is fairly constant with rotational speed. In the rotational direction, the journal bearings are stiffer than the roller and ball bearings. The journal bearing rotational stiffness also increases significantly with increasing rotational speed.

Figure 7 compares total damping in the radial direction for the journal bearings at varying rotational speeds. As a point of comparison, ball and roller bearing damping typically varies between 0.1 and 0.5 N/mm/s [18], values more than three orders of magnitude less than the damping in the journal bearings. Also, damping decreases slightly with increasing rotational speed for the journal bearing.

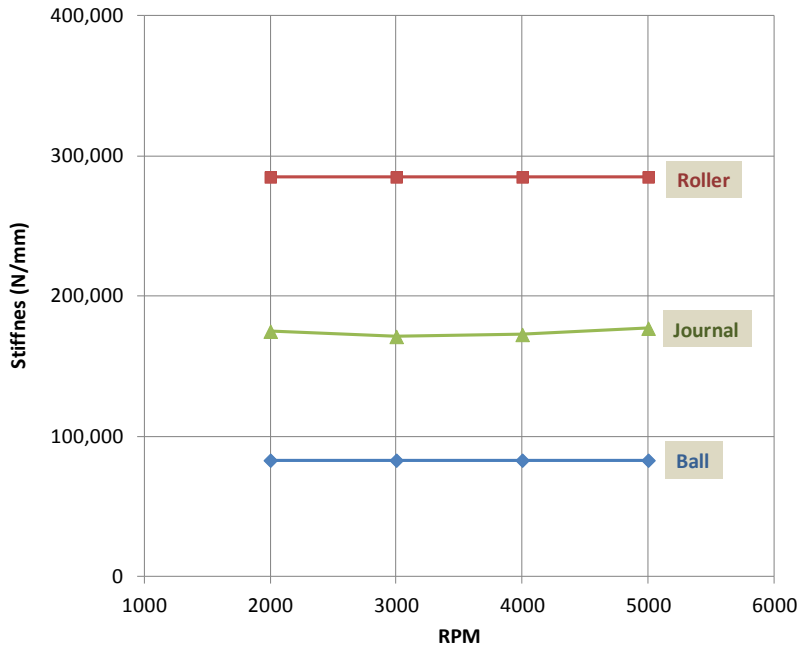

Figure 5: Comparison between journal bearing radial stiffnesses to those of ball and roller bearings at input side of gearbox at 700 in-lb torque.

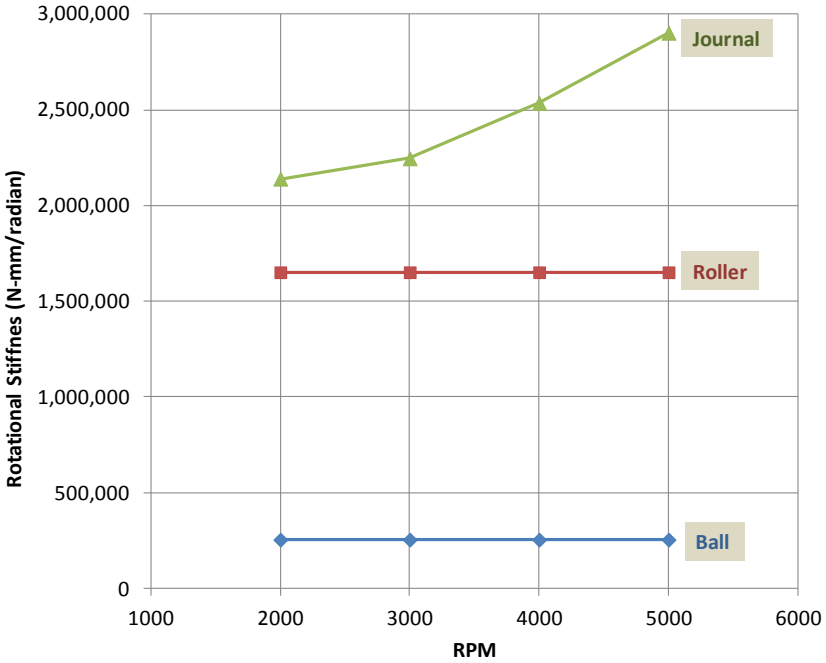

Figure 6: Comparison between journal bearing rotational stiffness magnitudes to those of ball and roller bearings at input side of gearbox at 700 in-lb torque.

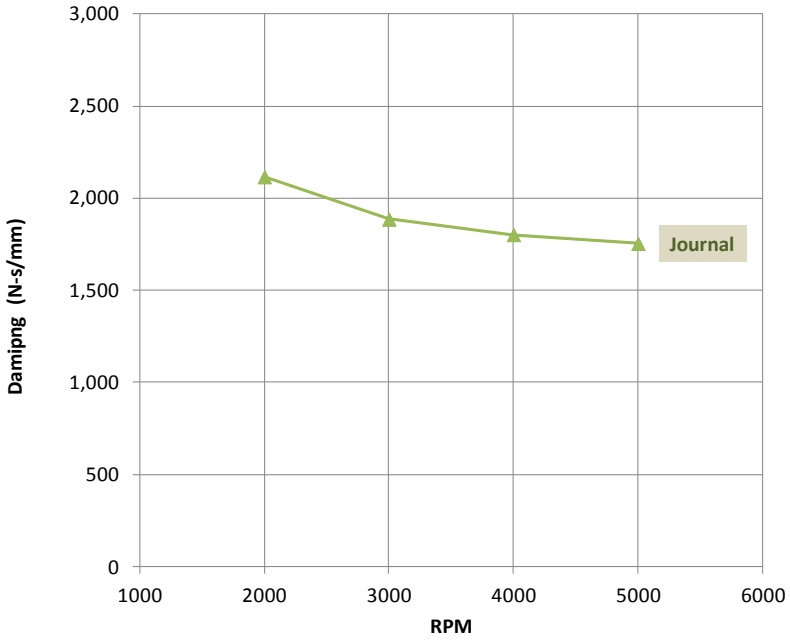

Figure 7: Journal bearing radial damping at 700 in-lb torque and variable rpm.

4 COMPONENT MODE SYNTHESIS CALCULATIONS ON A SIMPLE GEARBOX

ARL/Penn State's CHAMP approach (Computational Hydroacoustic Modeling Programs) [19], outlined in Figure 8, is based on CMS. Component modes of the gearbox and the shafting may be computed by a commercial FE code, such as NASTRAN, and stored. Next, CHAMP computes the forced response of the coupled system based on the component modes, and any combination of impedances which couple the component modes together. As described in the introduction, the CMS procedure is augmented with (1) residual vectors at the

bearing locations and (2) modes which are based on nominal bearing impedances (instead of the usual free boundary conditions).

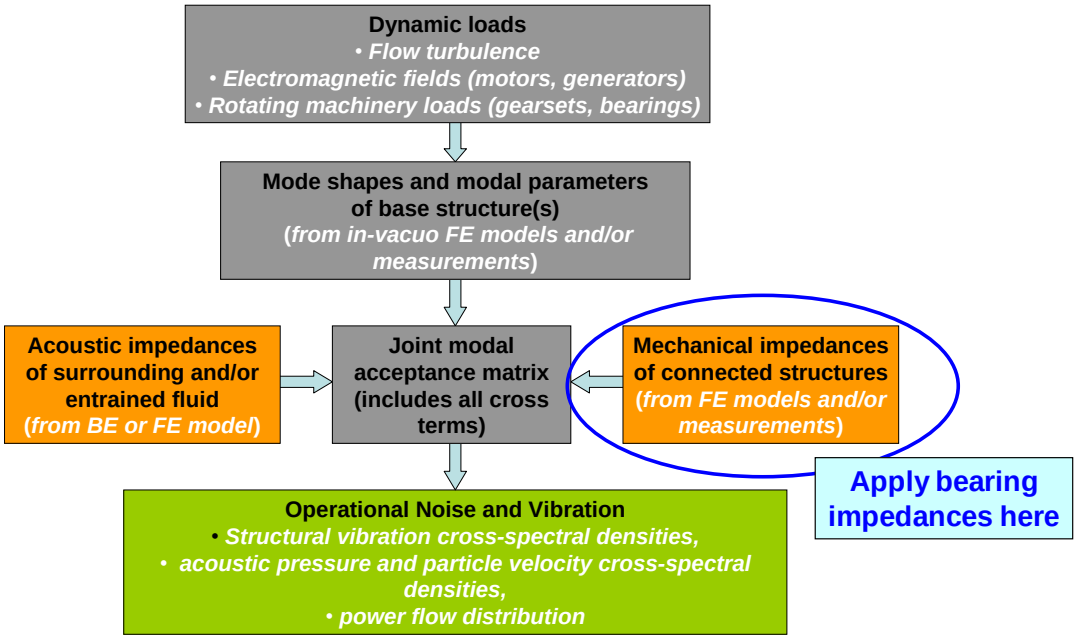

Figure 8: CHAMP noise and vibration simulation capability.

To evaluate the augmented CMS procedure, a simplified model with properties similar to those of the NASA GRC gearbox was constructed, as shown in Figure 9. The box dimensions and wall thicknesses are consistent with those of the NASA GRC gearbox, and a single shaft, modeled with beam elements, is inserted in the center of the box, and coupled to the box via a roller and ball bearing. The shaft is driven at its center, and the response of the shaft and housing top plate are computed both with CMS, and directly within NASTRAN (a direct, exact solution which does not rely on a modal series summation). Sample modes of the uncoupled box and shafting are shown in Figure 10. Note that the shafting is actually circular, but represented with a square cross section in the FE viewing software.

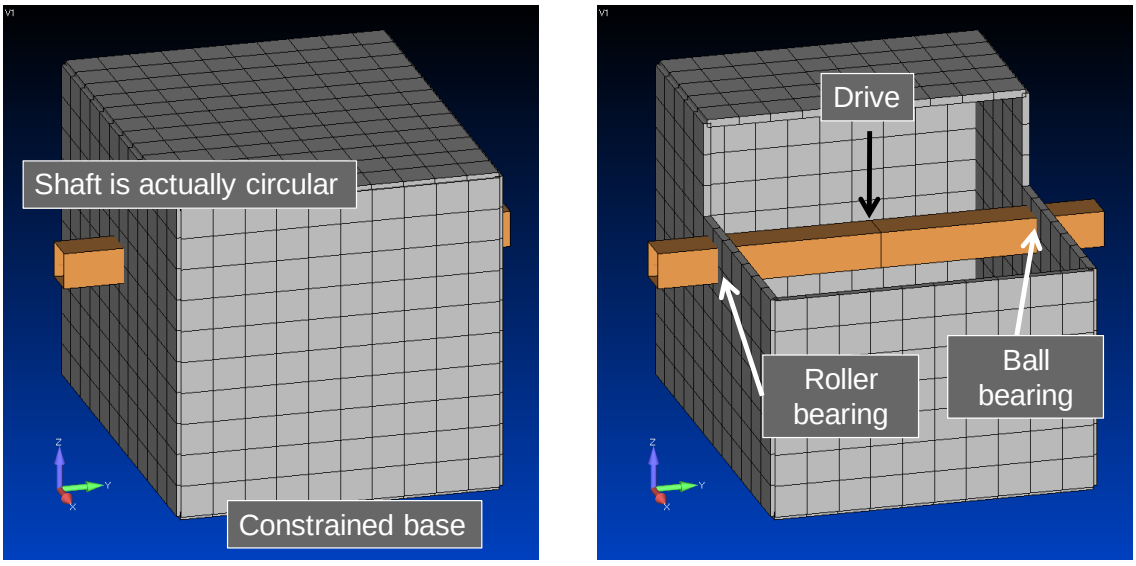

Figure 9: Finite element model of simplified gearbox with single shaft.

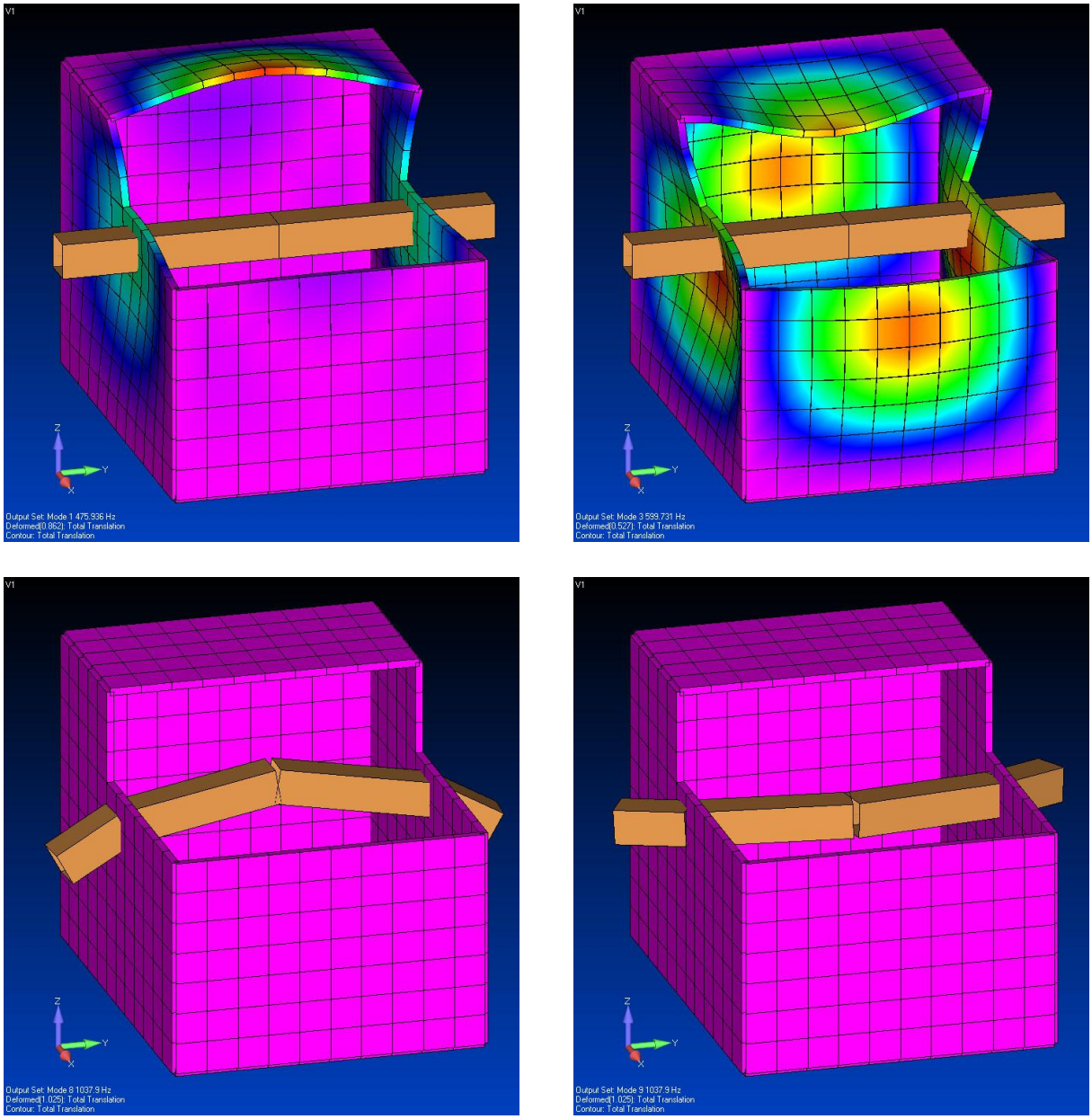

Figure 10: Sample mode shapes of housing (top) and shafting (bottom) of simplified gearbox model, free boundary conditions.

Figure 11 compares computed top plate vibration in response to a shaft drive. The 'actual stiffness' curve is the exact, direct solution, and the 'zero stiffness' curves are based on CMS solutions using free boundary condition modes with and without residual vectors. The CMS solutions used modes extracted for frequencies up to 4 Hz, or twice the frequency range of the analysis. When residual vectors are excluded from the solution, the CMS and exact results match only at a few selected resonance frequencies, and differ significantly at all other frequencies. Including the residual vectors leads to dramatic improvement in the CMS results. However, the CMS with residual vectors and exact results still do not match perfectly. To improve convergence, we therefore further modify the CMS procedure to use component modes which are based on including nominal bearing stiffnesses in the FE model.

The nominal bearing stiffnesses, which are set based on the computed rolling element and journal bearing stiffnesses over the ranges of operational speeds and torque conditions considered, lead to a set of component modes which are more similar to the actual modes

which occur under the various operating conditions. To correct the bearing stiffnesses to the actual values, the differences between the actual and nominal bearing stiffnesses are added or subtracted to the nominal values during the CMS process. This procedure, while efficiently allowing for rapid assessment of bearing changes, also allows for non-symmetric bearing stiffnesses to be accounted for easily, by using symmetric nominal stiffnesses to compute the component modes, and correcting to the actual non-symmetric bearing stiffnesses during the CMS analysis. Figure 12 compares the exact top plate vibration solution with a solution using nominal bearing stiffnesses (chosen here to be the average of the ball and roller bearing stiffnesses) and a solution using CMS and adjustments to the bearing stiffnesses (both also with residual vectors). The exact and CMS solution based on modes computed using nominal bearing stiffnesses are nearly identical.

5 SUMMARY AND CONCLUSIONS

An augmented CMS technique, using residual vectors and nominal bearing impedances, is demonstrated for transmission modelling. A simplified version of the NASA GRC test gearbox was used to verify the approach. The augmented technique leads to significant improvements in solution convergence compared to traditional CMS. The approach allows for rapid assessments of various bearing combinations and operating conditions.

The technique was later used to assess the noise and vibration performance differences in the actual NASA gearbox when switching from REBs to JBs. The numerical models and physical experiments indicate similar performance differences. For details, please see [14].

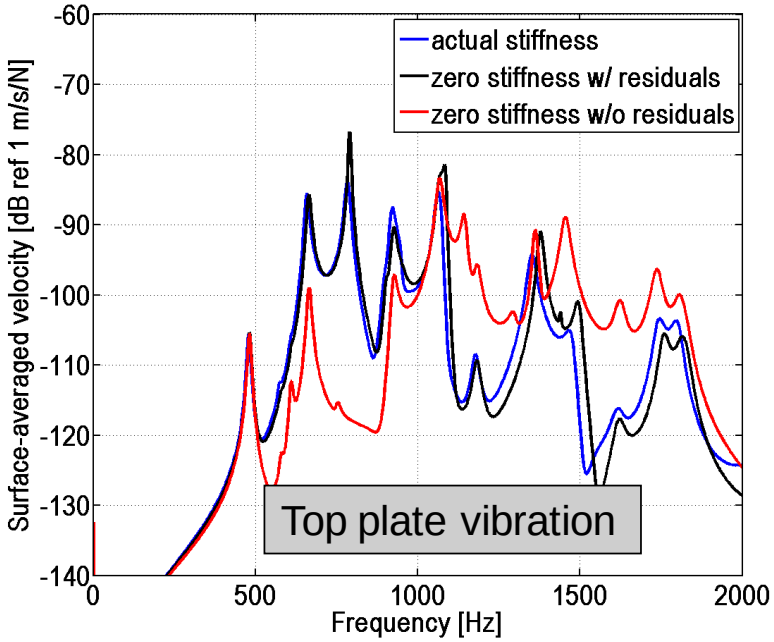

Figure 11: Top plate vibration of simple gearbox. 'Actual stiffness' curve is the exact solution, and ‘zero stiffness’ curves are based on CMS solutions with and without residual vectors.

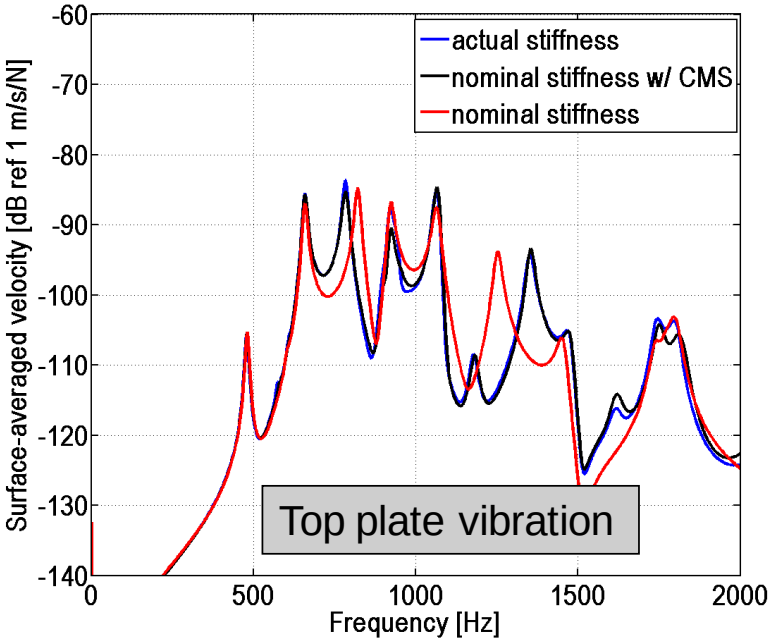

Figure 12: Top plate vibration of simple gearbox. 'Actual stiffness' curve is the exact solution, and 'nominal stiffness' curves are shown with and without CMS.

REFERENCES

[1] Sellgren, U., and Akerblom, M., "A model-based study of gearbox-induced noise," *NAFEMS Seminar: Component and System Analysis using Numerical Simulation Techniques*, 23-24 November 2005, Gothenburg, Sweden.

[2] Tanaka, E., Houjoh, H., Mutoh, D., Motoshiromizu, H., Ohno, K., and Tanaka, N., "Vibration and sound radiation analysis for designing a low-noise gearbox with a multi-stage helical gear system," *JSME International Journal, Series C*, 46 (3), 1178-1185, 2003.

[3] Soeiro, N.S., Gerges, S.N.Y., Jordan, R., and Arenas, J.P., "Numerical modeling of the vibro-acoustic behavior of a vehicle gearbox," *International Journal of Acoustics and Vibration*, 10 (2), 61-72, 2005.

[4] Abbes, M.S., Bouaziz, S., Chaari, F., Maatar, M., and Haddar, M., "An acoustic-structural interaction modeling for the evaluation of a gearbox-radiated noise," *International Journal of Mechanical Sciences*, 50, 569-577, 2008.

[5] Kartik, V., and Houser, D.R., "An investigation of shaft dynamic effects on gear vibration and noise excitations," *SAE paper 2003-01-1491*, 2003.

[6] Fleming, D.P., "Vibration transmission through bearings with application to gearboxes," NASA/TM-2007-214954, *Proceedings of the 4th Biennial International Symposium on Stability Control of Rotating Machinery (ISCORMA-4)*, Calgary, Alberta, Canada, 2007.

[7] He, S., Singh, R., and Pavic, G., "Effect of sliding friction on gear noise based on a refined vibro-acoustic formulation," *Noise Control Engineering Journal*, 56 (3), 164-175, 2008.

[8] Oswald, F. B., Seybert, A.F., Wu, T.W., and Atherton, W., "Comparison of analysis and experiment for gearbox noise," NASA Technical Memorandum 105330, *Proceedings of the 6th International Power Transmission and Gearing Conference*, Phoenix, Arizona, 1992.

[9] Hurty, W.C., "Dynamic analysis of structural systems using component modes," *AIAA Journal*, 3, 678-685, 1965.

[10] Craig, R.R., and Bampton, M.C.C., "Coupling of structures for dynamic analysis," *AIAA Journal*, 6, 1313-1319, 1968.

[11] MacNeal, R.H., "A hybrid method of component mode synthesis," *Computers and Structures*, 1, 581-601, 1971.

[12] Farstad, J.E., and Singh, R., "Effects of modal truncation errors on transmitted dynamic power estimates in discretely joined component assemblies," *Journal of the Acoustical Society of America*, 100 (5), 3144-3158, 1996.

[13] Rose, T., "Using residual vectors in MSC/NASTRAN dynamic analysis to improve accuracy," *Proceedings of the 1991 MSC World User's Conference*, 1991.

[14] Hambric, S.A., Hanford, A.D., Shepherd, M.R., Campbell, R.L., and Smith, E.C., *Rotorcraft transmission noise path model, including distributed fluid film bearing impedance modeling*, NASA/CR-2010-216812, September 2010.

[15] Lim, T.C., and Singh, R., "Vibration transmission through rolling element bearings, Part I: bearing stiffness formulation," *Journal of sound and vibration*, 139 (2), 179-199, 1990.

[16] Liew, H-V., and Lim, T.C., "Analysis of time-varying rolling element bearing characteristics," *Journal of Sound and Vibration*, 283, 1163-1179, 2005.

[17] Campbell, R.L., "Distributed Journal Bearing Dynamic Coefficients for Structural Finite Element Models," *Proceedings of ASME IMECE 2003*, NCA-43770, 2003.

[18] Kraus, J., Blech, J.J., and Braun, S.G., "In Situ determination of rolling bearing stiffness and damping by modal analysis," *ASME Journal of Vibration, Acoustics, Stress, and Reliability in Design*, 109, 235-240, 1987.

[19] Hambric, S.A., Boger, D.A., Fahnline, J.B., and Campbell, R.L., "Structure- and fluid-borne acoustic power sources induced by turbulent flow in 90 degree piping elbows," *Journal of Fluids and Structures*, 26, 121-147, 2010.